

MERLAB, PC

Mechanical Engineering Research Laboratory
357 S. Candler St.
Decatur, GA 30030-3746

David R. Smith, Ph.D., PE

David_Smith@merlab.com
(404)378-2138
FAX: (404)378-0822

TO: Mike Nolan**FROM:** David R. Smith**DATE:** May 8, 2007, (Rev 1 date May 29, 2007)**RE:** Analysis of Arecibo Elevation Wheel and Track Life**Summary and Disclaimer**

The elevation wheel and track interface at the Arecibo telescope shows obvious signs of wear. This wear takes many forms. Pitting is in clear evidence, both on the track wear plate rolling surface and on the wheels. Local cracking, both lateral and axial, is present at the mounting holes of the existing wear plate. Further, at some locations above failed rail joint butt welds, the track wear plate has failed completely due to a transverse crack. There is also evidence of scoring of the rolling surface, as well as breakage of the securing screws.

This document seeks to provide a baseline calculation of the stresses and expected load cycles at the wheel/rail interface. Based on this loading profile, predictions are then made concerning the expected lifetime of the wheel and the track wear plate. The results suggest that it should be possible for the wheels to reach infinite life without major changes, but that the track wear plate is likely to require periodic replacement. While the calculations have been made with care and are believed to be correct, MERLAB is not the system designer and cannot accept liability for any errors or omissions. As a result, any changes implemented in the field must first be reviewed and approved by the designer of the system.

Specific suggestions include repair and reinforcement of the butt weld joints in the supporting rail and an increase in the wheel crown radius to reduce the surface contact stresses. The present analysis also supports the improvements to the wheel design already made by field personnel at the observatory.

1.0 Relevant Documents

The following drawings and documents are relevant to this analysis:

1. Elevation Rail & Rack I: As-built Drawing S-24 by CRSI, dated 7-31-1996.
2. Gregorian Trolley I: As-built Drawing S-30 by CRSI, dated 8-31-1996.
3. Gregorian Trolley III: As-built Drawing S-32 by CRSI, dated 8-31-1996.
4. Gregorian Enclosure: As-built Drawing S-33 by CRSI, dated 8-31-1996.
5. Maldonado, J., Dome Weight, Technical Memo, March 28, 2003.
6. DIN 19704-1, Hydraulic Steel Structures – Part 1: Criteria for Design and Calculation.
7. Young, W., *Roark's Formulas for Stress and Strain*, 6th ed., McGraw-Hill, 1989.

2.0 Introduction

During a trip to the platform in late May (D. Smith and M. Nolan), we had the opportunity to perform a brief visual inspection of the wheel and track interface for the elevation support system. This inspection confirmed, as already reported, that there are several current problems with this system. The observed problems are as follows:

1. Pitting of the wear plate rolling surface.
2. Pitting of some of the wheels.
3. Transverse cracking of the wear plate at the holes for its securing bolts.
4. Axial cracking of the wear plate at some of the holes for its securing bolts.
5. Scoring of the wear plate.
6. Breaking of the securing bolts.
7. Complete transverse breakage of the wear plate at joints in the rail where the flange butt welds had failed.

Since the total weight of the Gregorian dome is known to be well above the original design specifications, and it is anticipated that this may have contributed to the relatively low lifetime of the components. The purpose of this document is to present the expected surface stresses and lifetimes of the wheels and the wear plate and to make recommendations about how to improve the situation.

3.0 General Geometry

As shown in the drawings, the Gregorian dome is held up by two trolleys. Each trolley is supported by eight wheels on each of two parallel rails. A system of three successive balance pivots ensures that the load on a given trolley is carried uniformly between the wheels on a given rail. Of course, the position of the center of gravity (CG) of the dome affects the load distribution between the two trolleys and between the two rails.

The dome position, defined here as the centerline between the two trolleys, is assumed to move from a minimum zenith angle (ZA) of 1° from the center of the elevation feed arm arc to a maximum of 19.7° . A schematic of the dome support geometry and the location of the CG is shown in Figure 1. For reference, the angle reported on the encoders refers to a location 1.1113° uphill from this dome position.

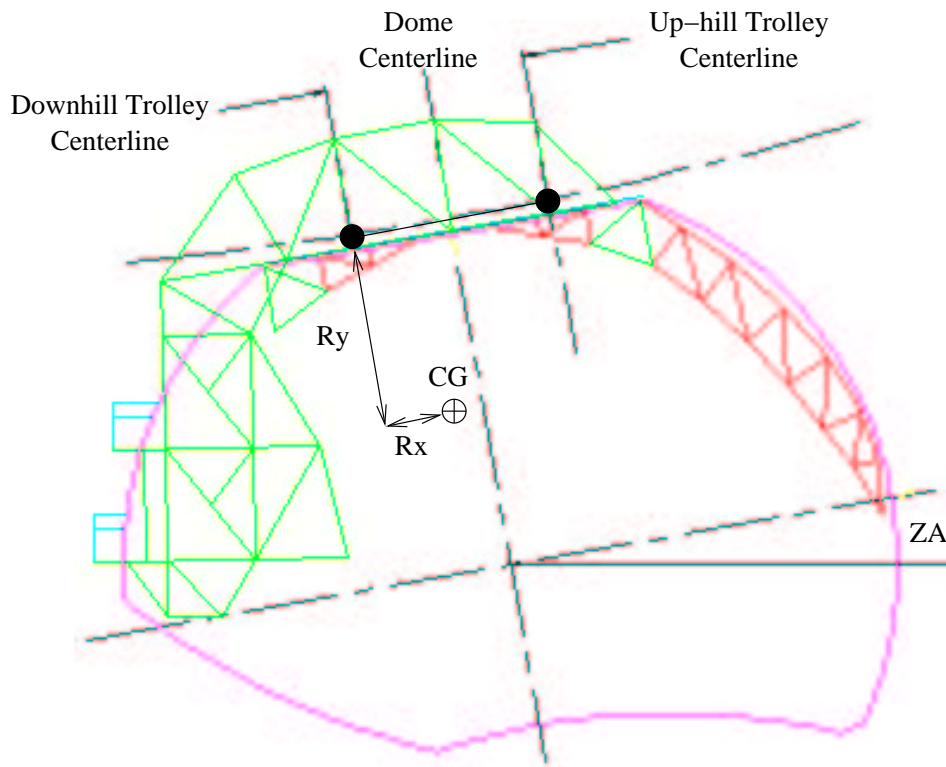


Figure 1: Gregorian Dome Layout

4.0 Forces and CG Location

The dome was weighed at each of its four pickup corners (the centerlines of the trolleys) in February of 2003, and the results were documented in a memorandum. The weights were obtained both by the jacks and by separate load cells. The memorandum reports the weights for corners 1–4, and it is assumed here that 1–2 are the weights for the up-hill trolley and 3–4 for the downhill trolley. All values include the trolley weights. In general, the two methods showed excellent agreement, except that the load cells showed significant variation between the two sides of the up-hill trolley. Since the total loads match well, for this document, we assume that the numbers from the jacks are correct. These are summarized in Table 1.

Table 1: Dome Weights (2/27/2003)

Corner Number	Trolley	Weight (lbf)
1	Up-hill	23,763.6
2	Up-hill	24,867.6
Total	Up-hill	48,631.2
3	Downhill	84,483.6
4	Downhill	82,275.6
Total	Downhill	166,759.2
Grand Total	Downhill	215,390.4

While the position of the dome is not reported in the memorandum, Phil Perillat reports that the dome angle, as measured at the encoders, was at a zenith angle of 1.05° for the entire day reported for the weighing.

The drive system connection to the dome/trolley system is supported separately from the trolleys and acts through a drag link. It is assumed to act purely tangentially, and on the line between the trolley centerlines. This results in a free-body diagram shown in Figure 2. The trolley resultant forces are assumed to act purely normal to the track rolling surface at the trolley centerline.

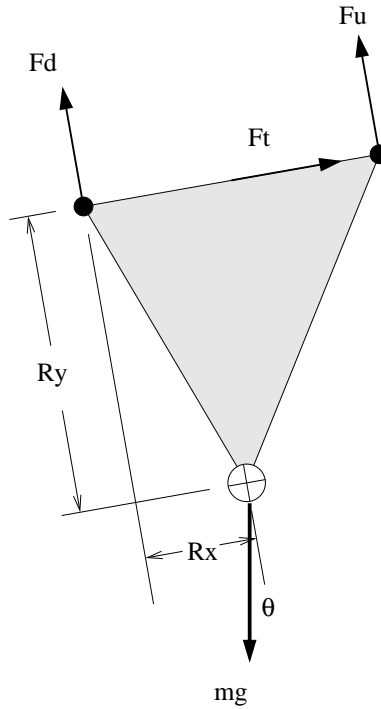


Figure 2: Free-Body Diagram

As the dome moves along the track, the suspended position of the CG causes the wheel forces to change. The measured distance between the trolley centerlines is shown by the drawings to be 21.5 ft, and the R_y position of the CG of the dome has been assumed (only by cursory inspection of the drawings) to be about 20 ft. The dome CG position in the direction of travel (R_x) can be calculated from Table 1, and is estimated to be about 4.5 ft up-hill of the downhill trolley centerline position (see Figure 2). The measured results also indicate that there is good left-right symmetry between the rails, though it is worth noting that the load cell results show substantial difference for the up-hill trolley (see Maldonado 2003).

The forces on the trolleys change as shown in Figure 3, with the equivalent wheel forces shown on the right hand vertical axis. To calculate the wheel forces, the whiffle-tree support is assumed to work perfectly and the two rails are assumed to carry equal load. Thus, the wheel loads within a trolley are 1/16th of the total trolley load.

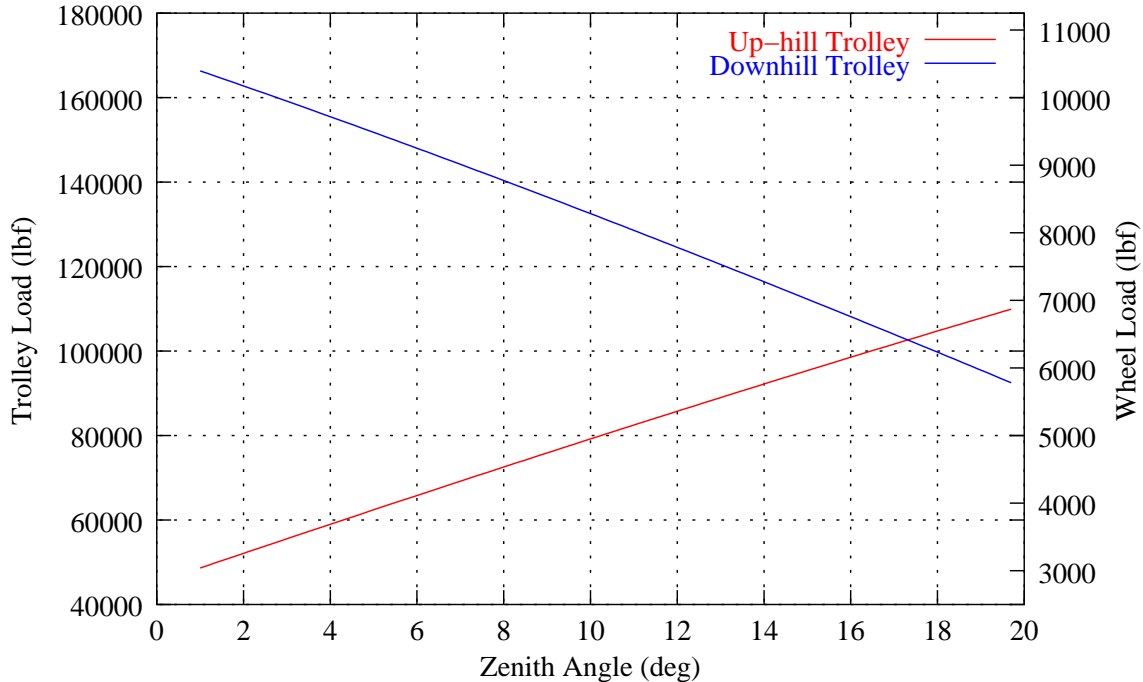


Figure 3: Expected Load Variation

The sensitivity of the wheel loads to the zenith angle position of the dome depends on the position R_y of the CG of the dome below the rail. At this time, no data has been provided concerning the actual value of this distance. To determine R_y , it would be necessary to lift the dome at two significantly different zenith angles, such as 1° and 10° . Such an experiment would allow direct calculation of the R_y CG location. Alternatively, strain gauging the trolley structure would allow measurement of this variation.

Generally, a load factor (or “factor of safety”) is applied to the expected dead load of a structure. In this document, when trying to explain known phenomena, no additional load factor is used. When making design recommendations, however, a load factor of 1.35 on the dead load has been applied.

Wind loads on the dome also affect the total load and the load distribution. These effects have not been taken into account in this analysis, but should be included in making final decisions on any design changes.

5.0 Number of Loading Cycles

In order to perform a fatigue (i.e., surface lifetime) analysis, it is necessary to know the expected number of cycles and the expected stresses. For purposes of this document, the following usage pattern for the telescope has been assumed:

Table 2: Track Usage Profile

One-way full length motions per day	11
One-way full length motions per year	4,000
One-way full length motions per 30 years	120,000

Of course, other usage patterns for the telescope, such as a large number of small switching motions at particular elevation angles, would imply different load cycling of the wheel and track.

5.1 Track Loading Cycles

The track loading is complicated, because as each wheel passes a given point, it does so at a different loading. As a conservative and more tractable analysis, the peak stress will be considered, but the number of load cycles for each point on the track must also be taken into account. As shown in Figure 4, the region of the each rail between dome positions of about 4–17°, see all 16 wheels with each full range motion of the dome. Most of the track falls into this worst-case number of cycles range, and the upper section would be expected to see the highest stresses.

For this worst-case number of cycles, the loading pattern is as shown in Table 3 below. For this number of cycles, the track rolling surface does not need to reach “infinite” life, but it is not short enough to be in the low-cycle (non-fatigue) limit.

Table 3: Track Loading Cycles

Track load cycles per day	176
Track load cycles per year	64,000
Track load cycles per 30 years	$\sim 2 \times 10^6$

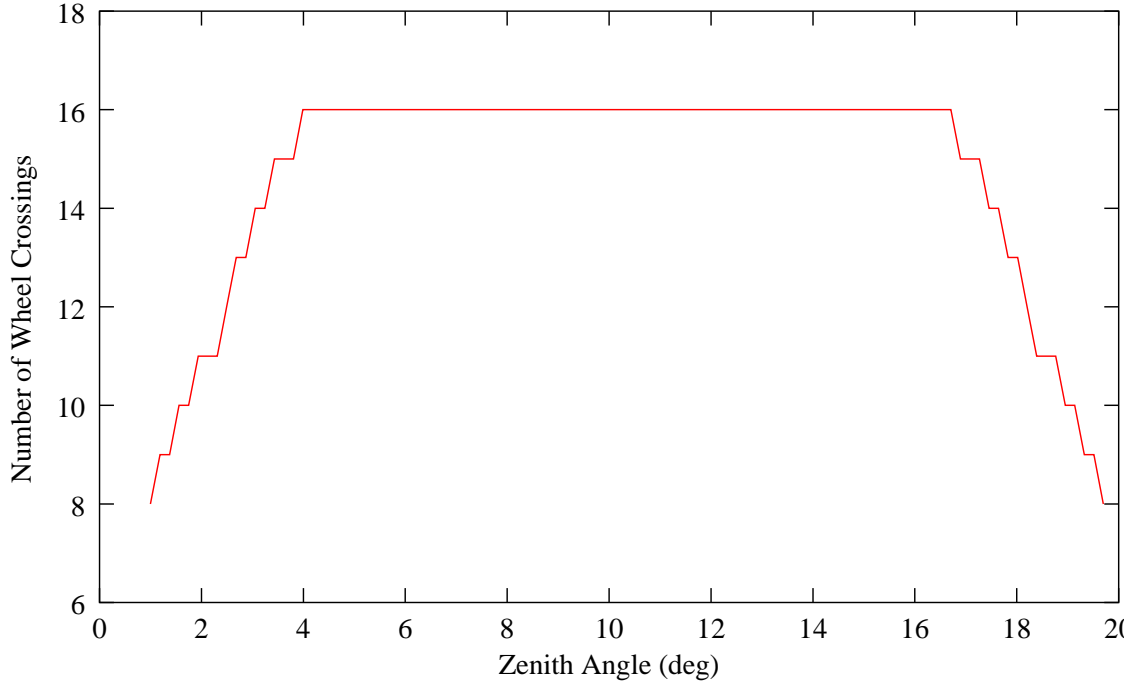


Figure 4: Number of Wheel Passages vs Zenith Angle

5.2 Wheel Loading Cycles

Since the wheels complete many revolutions as they roll along the track, each point on the wheel surface sees many more cycles than an individual track. According to drawing S-32, the wheels have a diameter of 6", and the track has a radius of 420'. This indicates a ratio of 1,680:1 between them. Thus, for each full range motion of 18.7° on the track, the wheels must rotate 87.27 times. This implies that the wheel surface must survive the following number of load cycles:

Table 4: Wheel Loading Cycles

Wheel cycles per day	960
Wheel cycles per year	350,000
Wheel cycles per 30 years	$\sim 10.5 \times 10^6$

Such high numbers of cycles suggest that the wheels should be designed for infinite life.

6.0 Contact Stresses

6.1 Rolling Surface Geometry and Material Properties

In the stress and life calculations, the several material properties and dimensions are important. The relevant dimensions are the radius of the wheel, R_1 , the crown radius of the wheel, R'_1 , and the radii of curvature of the top surface of the track, R_2 , and R'_2 . These are summarized as follows:

$$\begin{aligned}
 R_1 &= 3 \text{ in} = 76.2 \text{ mm} \\
 R'_1 &= 5 \text{ ft} = 60 \text{ in} = 1,524 \text{ mm} \\
 R_2 &= -420 \text{ ft} = -5,040 \text{ in} = -128,016 \text{ mm} \\
 R'_2 &= -\infty
 \end{aligned} \tag{1}$$

The relevant material properties are the modulus of elasticity of the wheel and rail (E_1 and E_2 , respectively), and their Poisson's ratios (ν_1 and ν_2 , respectively). Finally, it is useful to define a coefficient C_E based on these values. For steel wheels on steel rails, these values are as follows:

$$\begin{aligned}
 E_1 &= E_2 = 200,000 \text{ N/mm}^2 \\
 \nu_1 &= \nu_2 = 0.3 \\
 C_E &= \frac{1 - \nu_1^2}{E_1} + \frac{1 - \nu_2^2}{E_2}
 \end{aligned} \tag{2}$$

6.2 Contact Stress Calculation

The stresses here have been calculated according to Roark and Young (1989). In this formulation, it is convenient to define a constant K_D , such that

$$K_D = \frac{1.5}{1/R_1 + 1/R_2 + 1/R'_1 + 1/R'_2}. \tag{3}$$

Then, for a wheel load, P , the half-widths of the elliptical contact patch (c and d) are as follows:

$$\begin{aligned}
 c &= \alpha \sqrt[3]{PK_D C_E} \\
 d &= \beta \sqrt[3]{PK_D C_E}
 \end{aligned} \tag{4}$$

where α and β are constants determined from a table. The table is indexed based on a quantity called $\cos \theta$, which is defined as

$$\cos \theta = \frac{K_D}{1.5} \sqrt{\left(\frac{1}{R_1} - \frac{1}{R'_1}\right)^2 + \left(\frac{1}{R_2} - \frac{1}{R'_2}\right)^2 + 2\left(\frac{1}{R_1} - \frac{1}{R'_1}\right)\left(\frac{1}{R_2} - \frac{1}{R'_2}\right) \cos 2\phi}$$

where ϕ is the angle between the plane of the radius of curvature R_1 and the plane of the radius of curvature R_2 . In this case, $\phi = 0$, and $R'_2 = \infty$, so

$$\cos \theta = \frac{K_D}{1.5} \left(\frac{1}{R_1} - \frac{1}{R'_1} + \frac{1}{R_2} \right) = 0.9047.$$

Interpolating from the table in Roark and Young, $\cos \theta = 0.9047$ corresponds to

$$\begin{aligned} \alpha &= 3.164 \\ \beta &= 0.456 \end{aligned} \tag{5}$$

Once the size of the contact ellipse is calculated, the maximum stress is determined by the relation

$$p_{\max} = \frac{1.5P}{\pi cd}.$$

The results for varying values of applied wheel load P are summarized in Table 5 below. The table includes the contact patch dimensions and the contact stresses. The stresses are given both in psi and in MPa.

Table 5: Contact Patch Dimensions and Stresses

Wheel Load P (lbf)	Major Axis $2c$ (in)	Minor Axis $2d$ (in)	Contact Stress p_{\max} (psi)	Contact Stress p_{\max} (MPa)
2,000	0.515	0.074	100,100	690
4,000	0.649	0.093	126,100	870
6,000	0.742	0.107	144,400	995
8,000	0.817	0.118	158,900	1,096
10,000	0.880	0.127	171,200	1,180
12,000	0.935	0.135	181,900	1,254
14,000	0.985	0.142	191,500	1,320
16,000	1.030	0.148	200,200	1,380

The contact stresses as a function of wheel load are shown graphically in Figure 5, and the contact patch widths vs wheel load are shown in Figures 6–7. Finally, the expected

wheel contact stresses for the upper and lower trolley as a function of zenith angle are shown in Figure 8.

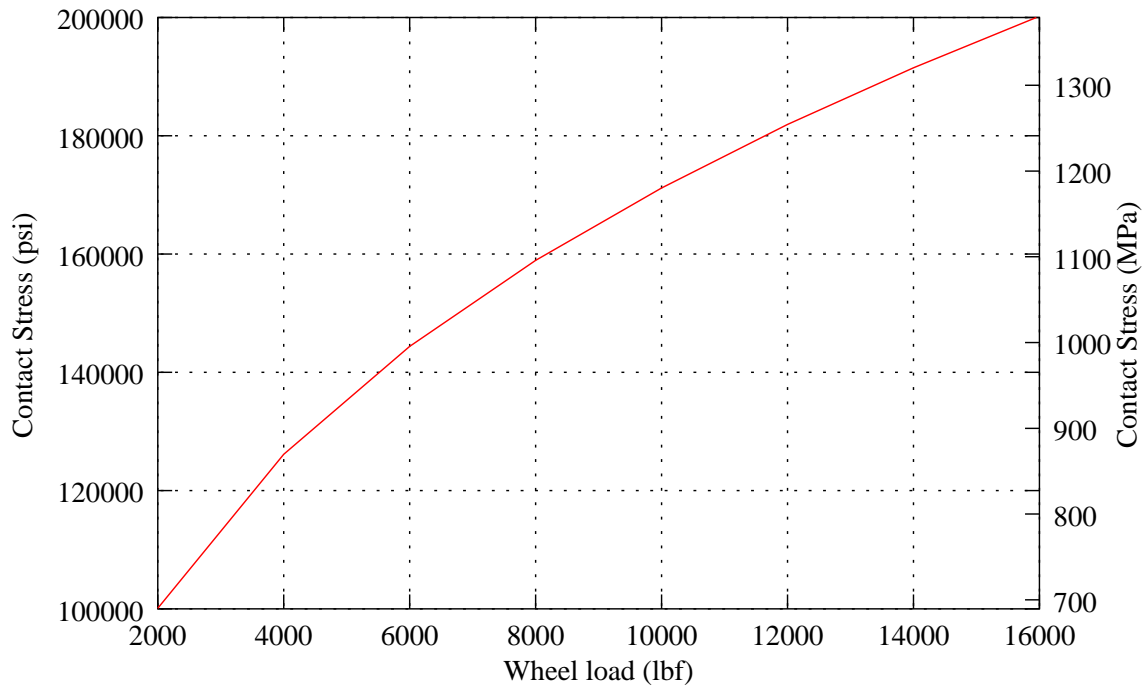


Figure 5: Contact Stress as a Function of Wheel Load

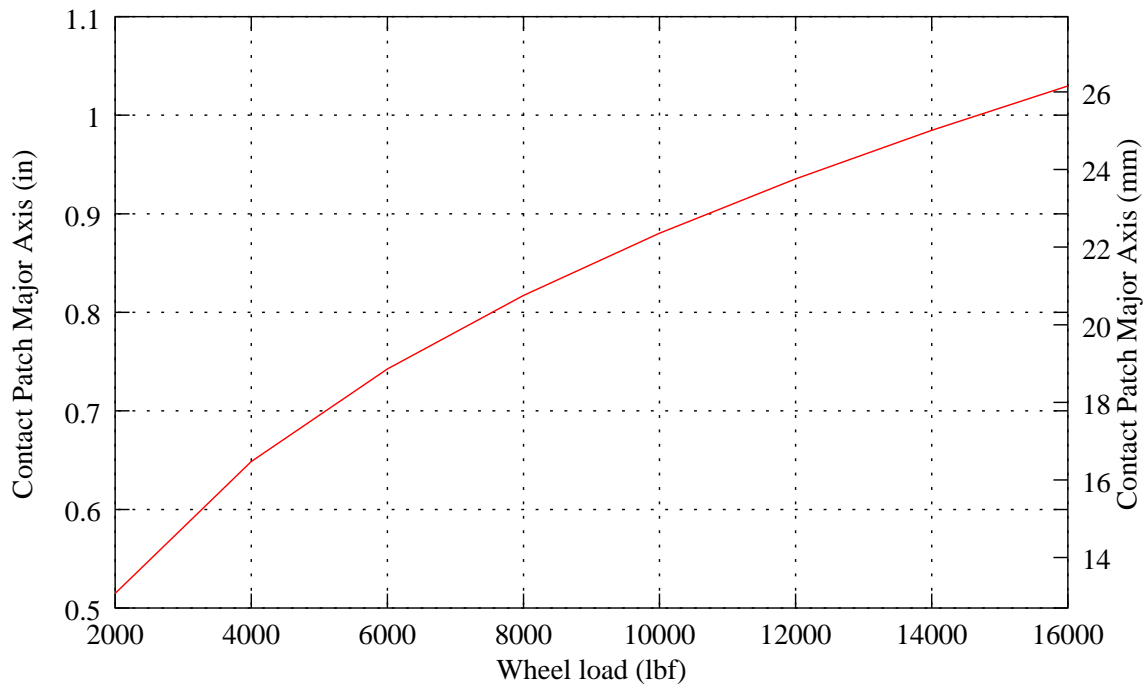


Figure 6: Contact Patch Major Axis vs Wheel Load

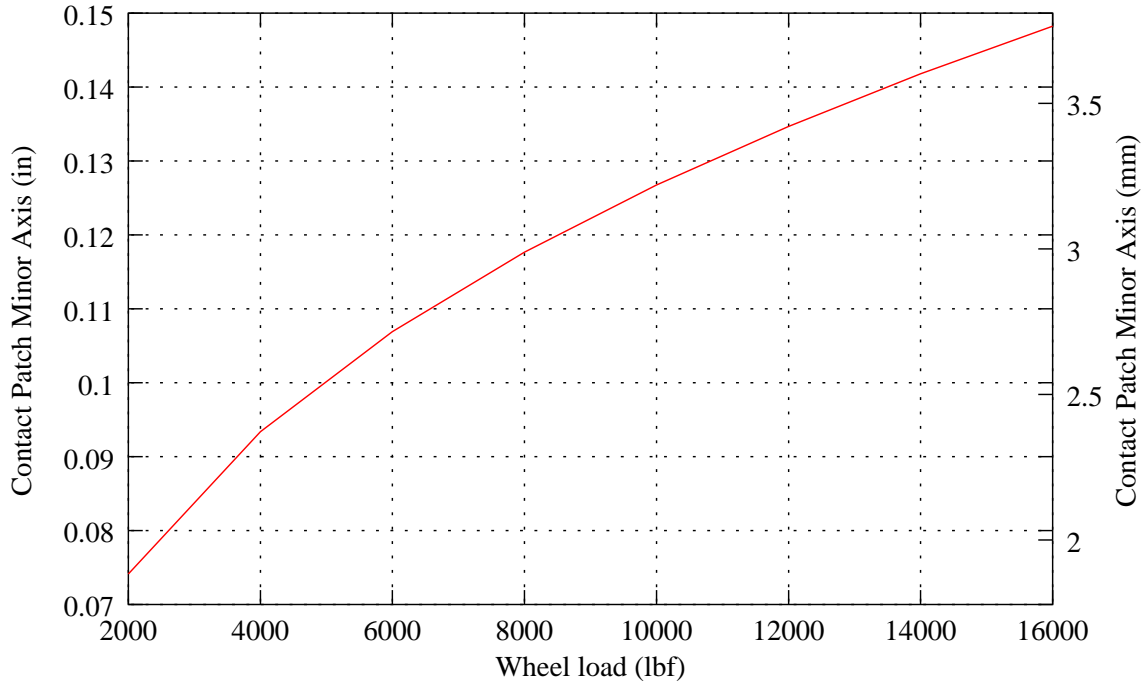


Figure 7: Contact Patch Minor Axis vs Wheel Load

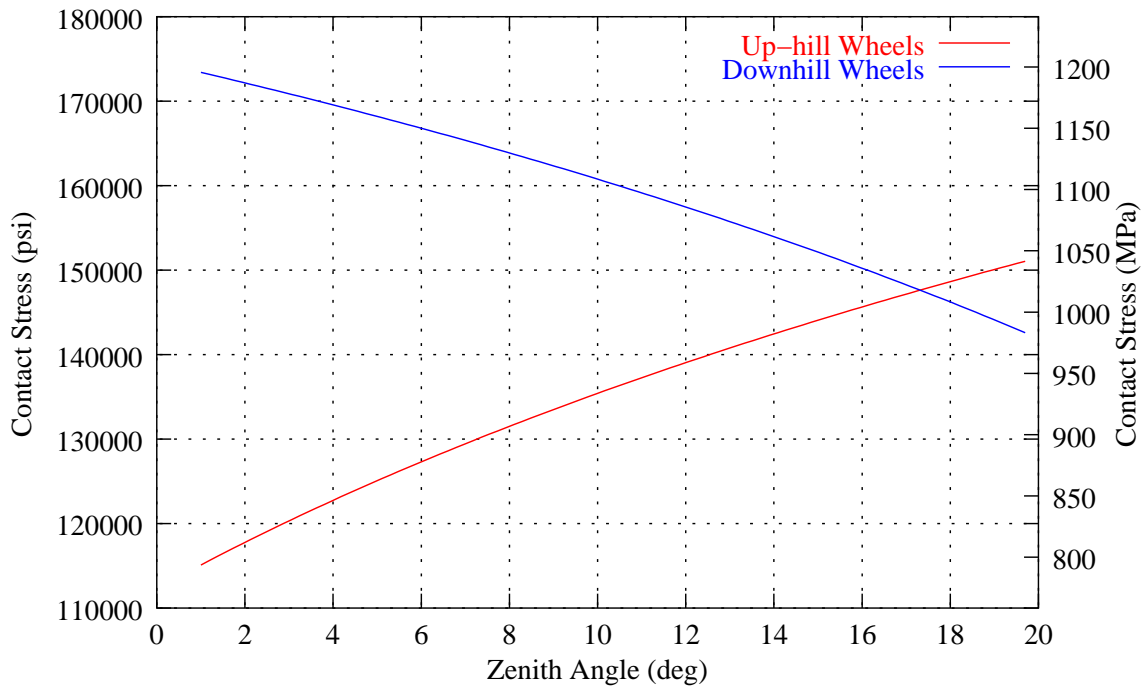


Figure 8: Expected Wheel Stresses vs Zenith Angle

7.0 Expected Lifetime of the Rolling Interface

In order to determine the expected lifetime of the rolling surface (or, equivalently, to determine the required surface hardness for a desired lifetime), an appropriate standard to use is DIN 19704-1. This standard includes design criteria for wheels rolling on rails in large cranes (Note: MERLAB does not have a copy of the standard itself, and is instead quoting formulas used by MT-Mechatronics in the design of the LMT azimuth wheel and track interface). Since these structures are large and slow, they are an appropriate analog for telescope wheel and track designs. According to the guidelines from DIN 19704-1 for wheels rolling on rails, the maximum allowable contact stress, p_{allow} , for a given material is given by the relationship

$$\begin{aligned} p_{\text{allow}} &= 6.0H & \text{for } N < 62,500 \\ p_{\text{allow}} &= 3.0H \sqrt[5]{\frac{2 \times 10^6}{N}} & \text{for } 62500 \leq N \leq 2 \times 10^6 \\ p_{\text{allow}} &= 3.0H & \text{for } N > 2 \times 10^6 \end{aligned} \quad (6)$$

where H is the Brinell hardness of the material, N is the number of cycles, and p_{allow} is given in units of MPa. The standard is not specific on whether the resulting lifetime prediction is before or after the onset of pitting, but these are the values given in the standard for design.

Using this equation, it is also possible to estimate the available life given the hardness of the material and the actual contact stress (p_{max}), using the following equation:

$$N = 3^5 H^5 \frac{2 \times 10^6}{p_{\text{max}}^5} = 4.86 \times 10^8 \frac{H^5}{p_{\text{max}}^5}. \quad (7)$$

7.1 Wheel Lifetime

While the wheels are subject to varying load (see Figure 8), conservative application of the standard would use the maximum stress. For the wheel hardness called out in S-30 (360 BHN), and the maximum contact stress calculated above (1,200 MPa), the expected lifetime is about 1.2 million load cycles, or about 3.5 years. Felipe Soberal has reported that the actual wheels in the field are made from improved material (AISI 4140 instead of AISI 1045) and that they were specified with higher hardness (400 BHN). For this minimum hardness, the lifetime should already be beyond the endurance limit, so one would not expect to see the pitting evident on some wheels.

For design purposes, standards typically assume a load factor of 1.35 on the dead loads. Applying this factor to the expected wheel loads on the dome results in the wheel

stresses shown in Figure 9, with a maximum value of about 1,320 MPa. This suggests that an appropriate design hardness for the wheel should be of order 440 BHN for the wheels to have infinite life if the wheel geometry is kept the same.

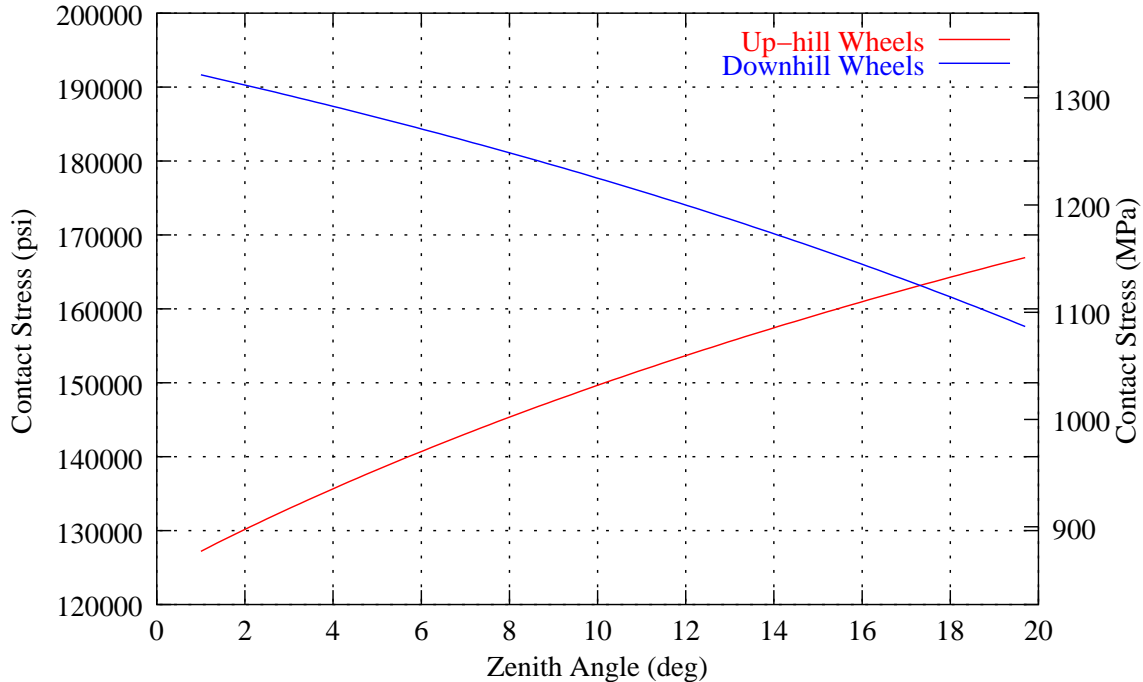


Figure 9: Expected Wheel Stresses vs Zenith Angle, FS=1.35

7.2 Track Lifetime

The stresses are the same for the track, except when the contact patch crosses one of the holes for the track mounting screws. At these points, there is a free edge in the material, which results in a stress concentration. While the literature is scarce on the effects of holes in the middle of the wheel path, some work with free-surface cracks suggests that the effective stress concentration factor is at least 1.5. This means that, for the actual stress predictions of about 1,200 MPa, the stress near the free surface of the hole could be 1,800 MPa, requiring a local hardness (through the full depth) of 600 BHN. For the design case that includes the load factor of 1.35, the maximum stress is 1,320 MPa, suggesting a stress near the hole of almost 2,000 MPa and a required hardness of 660 BHN. These values are impractical to achieve, and may even be beyond the ranges assumed in the standard.

For the hardness specified in drawing S-24 for the track (340 BHN), the expected lifetime according to DIN 19704-1, in load cycles, according to the assumed motion profile and expected loading is shown in Figure 10. Combining the effects of the upper and lower trolley (using the Miner-Palmgren relation) allows calculation of an estimate for the lifetime of the track in terms of full range motions of the dome. Using the motion profile

from Table 2, this can be converted to a number of years based on 4,000 one-way full range motions per year. These results are shown in Figure 11.

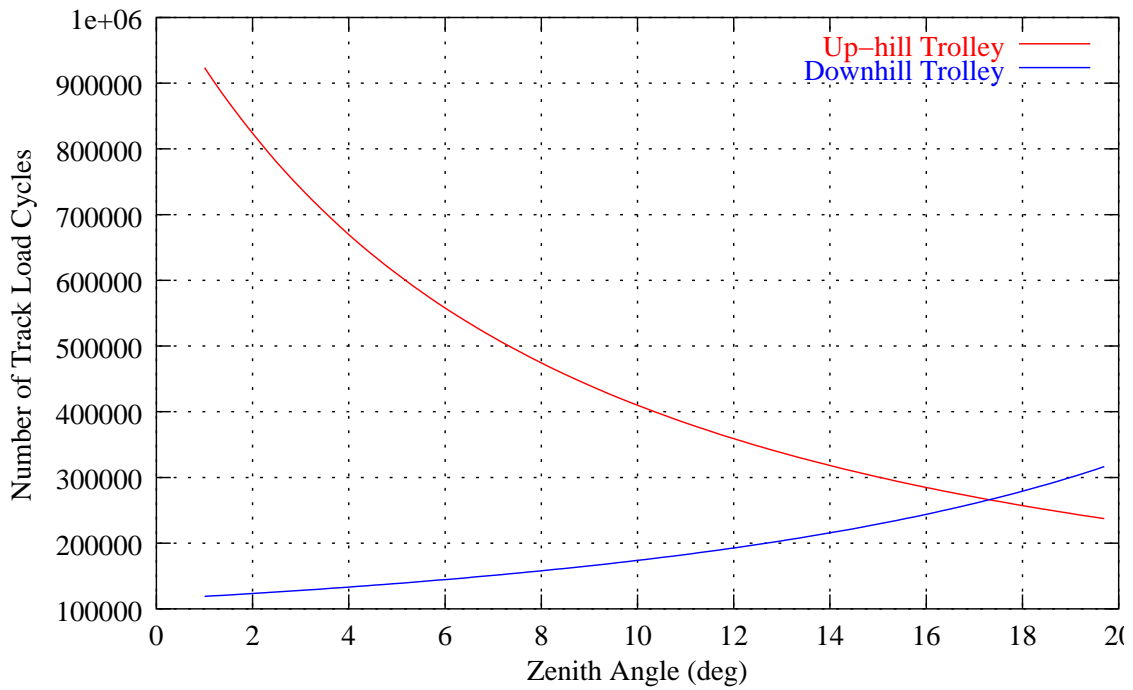


Figure 10: Allowable Load Cycles for Each Trolley

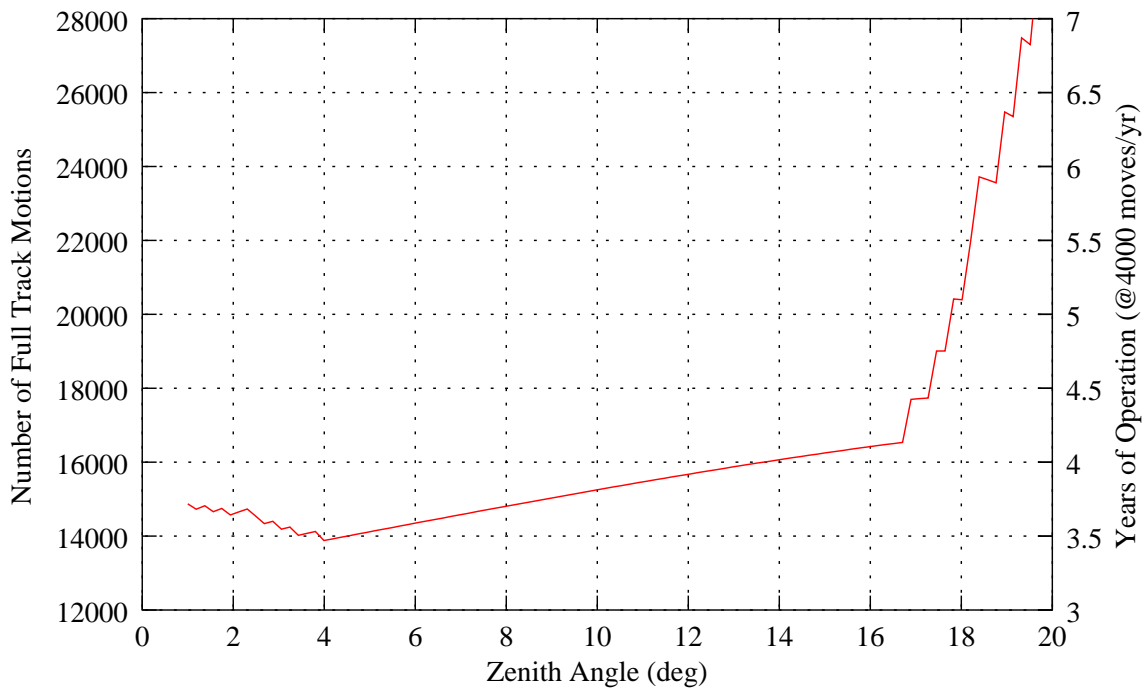


Figure 11: Estimated Track Lifetime

For design purposes, the load factor of 1.35 should be included, which results in the reduced track lifetime estimate shown in Figure 12.

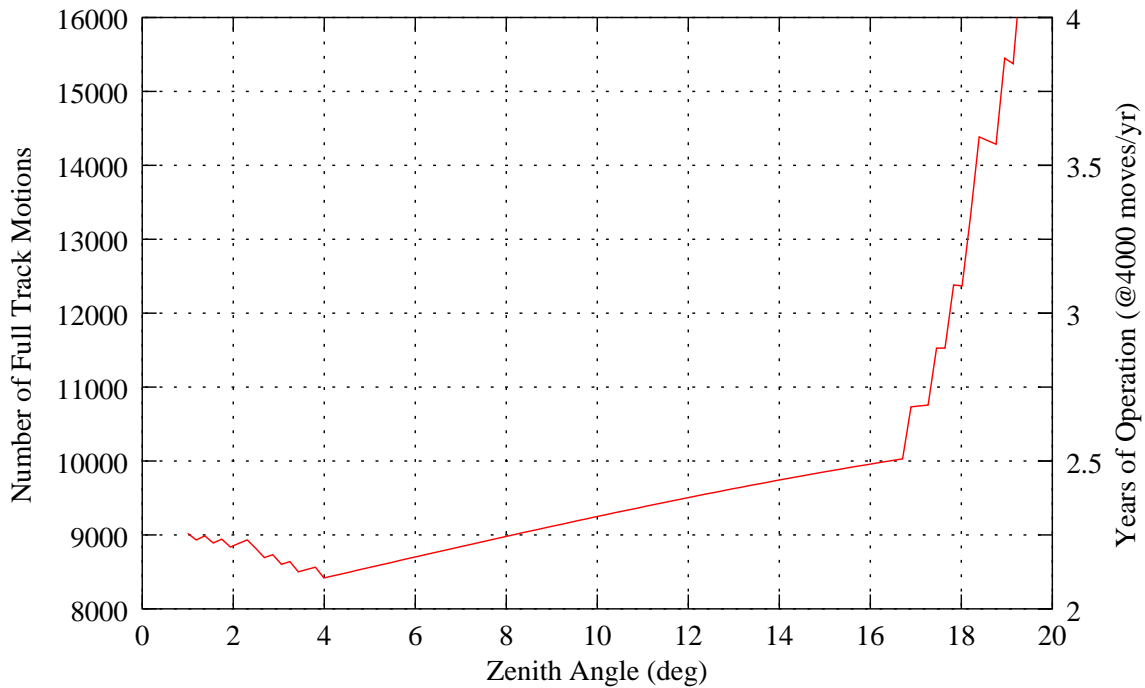


Figure 12: Estimated Track Lifetime, FS=1.35

7.3 Comparison to Railway Standard

According to Roark and Young (1989), the American Railway Engineering Association recommends the following allowable line load, in lbf/in, for a cylindrical wheel of this diameter on a flat rail:

$$P = \frac{S_y - 13000}{20000} 600d, \quad (8)$$

where S_y is the yield limit of the material in psi and d is the wheel diameter in inches. Since the geometry at Arecibo is neither a flat rail nor a cylindrical wheel, this standard cannot be applied directly. Further, it provides no information on the expected lifetime of the surface. However, it should provide a ballpark check on the more detailed analysis above.

Since the contact patch width is about 0.8 inch, $0.8P$ is approximately the total load. However, since the wheel is crowned, the peak stresses in the center of the patch are about 30% higher than for a uniformly distributed cylinder (based on a peak stress calculation for a cylinder and the actual geometry at 10,000 lbf wheel load). For this

case, d is 6 in, and S_y is likely on the order of 80,000 psi for the 1045 steel rail. This suggests a maximum recommended line load of about $P=12,000$ lbf/in, or a uniformly-loaded cylindrical total wheel load of 9,600 lbf. Assuming that the $\sim 30\%$ peak stress increase is valid over the actual wheel loading conditions, this corresponds to an allowable wheel load of order 7,400 lbf. Even without the stress concentration effects in the track, this estimate confirms that the track would be operating in a limited lifetime loading condition.

8.0 Interpretation of Results and Relation to Field Observations

8.1 Wheels

The wheel design shown in drawing S-32 would not be expected to have infinite life, even based only on the contact stresses. The actual design in use according to Felipe Soberal, however, should be adequate. Visual inspection and comments from the maintenance crew reveal that even these improved wheels have some problems with pitting, and that some wheels have even failed due to radial cracking. Metallurgical testing of the broken wheels indicates improper heat treatment. However, the existing wheels have not yet been sent out for testing, so there is no data on their material properties.

The analysis here has not taken into account either the traction forces or the skew forces due to small roller misalignments. These can be significant. As a result, if changes to the wheel material or heat treatment are considered in the future, upgrading them to the level required for the load factor of 1.35 should be considered. Alternatively, as discussed in section 9, the current material specifications should be sufficient if a larger crown radius is employed. In any event, bringing the wheels to the endurance limit (infinite life) appears feasible.

8.2 Track

From the investigation into the lifetime of the track, several features are evident.

1. For the measured weight distribution of the system, the lower part of the track would be expected to be in the worst surface condition.
2. The area around 4° dome angle position would be expected to have the shortest life, but not significantly different than most of the track up to about 15° .
3. The holes in the wheel path increase the stress such that a simple change in material will not make the track last indefinitely. Thus, the track will continue to be an item that needs periodic maintenance and replacement.

8.3 Other Comments Concerning Field Observations of the Track

While the lifetime calculation and stress concentration issues may explain the pitting on the track rolling surface a wheels, as well as the cracking at the holes. It does not address the final three issues observed at the platform. These are listed below, together with a brief discussion.

8.3.1 Scoring of the wear plate

Scoring of the wear plate is likely due to foreign material getting between the wheel and track. Given the age of the track, the clear evidence of cracking and pitting, and the presence of corrosion materials, this is not surprising. This effect could be reduced by installing a brush ahead and behind each wheel, or at least each pair of wheels.

8.3.2 Breaking of the securing bolts

There is evidence of breakage of the securing bolts. This is not surprising, given that the compression of the plate near the bolts as the wheel passes over them causes cyclic loading of the bolts. Additionally, it is likely that the track plate is sliding with respect to the supporting flange on the main beam and that the resulting shear loads may be causing shear fatigue of the bolts. Without changing the design of the track, the following actions may reduce the chances of bolts breaking.

1. Preload the bolts to 90% of their proof strength. These are 5/16"-18 machine screws, so they should have a tensile area of 0.0524 in². For a grade 8 bolt (proof strength of 120 ksi), these should be pre-loaded to about 5,600 lbf, which corresponds to a pre-load torque of about 30 lbf-ft. High preload should help prevent loosening and help to limit the slip between the plate and its supporting flange.
2. Use nuts with nylon inserts to resist loosening cause by the repeated wheel passages across the bolts.

Since the site engineering team reports that these measures are already in place, it may be necessary just to view the bolts as maintenance items. That is, monitor bolts for loosening or for breakage. The use of torque-striping paint on the nuts will speed inspection. If any bolts are found to be broken, all should be replaced, as it may indicate that others are nearing their fatigue limit.

8.3.3 Transverse breakage of the track plate

The transverse breakage of the track plate where the butt welded joints of the support rail have broken suggest that the flange is deflecting even beyond the normal bending and torsional beam behavior of the rail. This suggests that the flange is acting as a plate when the wheels pass, and that field reinforcement of the weld is appropriate. This should be checked with the designer to avoid any unexpected problems caused by increasing the local stiffness.

9.0 Recommendations

The materials problem for the wheel, and the stress concentration issue at the rail both would be less severe if the stress at the rolling interface were reduced. This can be accomplished either by opening up the crown radius on the wheels, making the wheels larger, or both. In order to make minimum changes to the geometry, the least invasive approach is to increase the crown radius. In the current design, according to drawing S-32, the crown radius is 5 ft for a 3 in radius (0.25 ft) wheel. This is a 20:1 ratio, and results in a contact patch width of less than an inch. Given the track width of 2.5 in, and given the apparent good alignment of the wheel system, as evidenced by the grease trail on the track, there is room for additional contact.

Increasing the crown radius to 10 ft would increase the contact patch width by about 30% and lower the stresses (even with the load factor of 1.35 applied) to a maximum of 1,130 MPa, which is 15% lower than the current condition.